Demonstration of improved beam quality in an image-rotating optical parametric oscillator

Darrell J. Armstrong and Arlee V. Smith

Department 1118, Sandia National Laboratories, Albuquerque, New Mexico 87185

Received July 23, 2001

We performed laboratory and numerical modeling studies of an optical parametric oscillator with 90° intracavity image rotation. We found that the signal beam was more symmetric than that from comparable cavities without image rotation, and it had low values of the beam quality factor, M^2. Oscillator performance agreed well with our numerical model. © 2002 Optical Society of America

OCIS codes: 230.4320, 190.4970.

One limitation of nanosecond optical parametric oscillators (OPOs) is difficulty in achieving good beam quality at high pulse energies. The necessary combination of short cavities and large beam diameters usually results in poor beam quality. In a previous paper, Smith and Bowers presented results of numerical simulations of image-rotating OPOs that indicated that walk-off between the signal and idler beams in the nonlinear crystal, combined with 90° image rotation of the resonated wave, could yield high-quality, symmetric signal beams.[1] In this Letter we present what are believed to be the first laboratory studies of such an OPO, corroborating those claims.

Figure 1 shows our OPO. The 15-mm-long KTP crystal is cut for type II collinear phase matching of 532 nm ↔ 800 nm + 1588 nm at $\theta = 58°$ in the xz plane. The 532-nm pump and 1588-nm idler are o polarized. The e-polarized 800-nm signal wave has a birefringent walk-off angle of 48 mrad, giving a displacement of 0.72 mm in the plane of the cavity on each crystal pass. This walk-off is comparable to the FWHM pump-beam diameter of 1.24 mm. The OPO cavity contains a Brewster-angled Dove prism rotated 45° to the plane of the ring. The three mirrors invert the image of the circulating signal beam in one plane on each cavity pass, and the Dove prism inverts the image about a plane parallel to its base. The combination of these two inversions is equivalent to a 90° image rotation on each cavity pass.

The OPO is singly resonant at 800 nm with an output coupling of 16% and is approximately 150 mm in length. We inject 30 mW of 800-nm light to induce single-longitudinal-mode oscillation. The OPO cavity length is stabilized to resonate the seed by use of locking electronics driving a piezoeletric mirror mount. The half-wave plates bracketing the Dove prism rotate the signal polarization between the plane of the cavity and the p plane of the Brewster-angled prism faces. The Nd:YAG pump laser is injection seeded for single-longitudinal-mode oscillation and has a pulse duration of 8 ns. The 532-nm pump beam is spatially filtered and has a slightly elliptical profile, with $1/e^2$ diameters of 2.1 mm × 2.3 mm.

Unlike a cavity composed of two parallel flat mirrors, a 90° image-rotating cavity with flat mirrors possesses a unique axis. A ray propagating along this axis overlaps itself after a single cavity pass, whereas a ray displaced laterally from the axis overlaps itself after four passes. In the laboratory we define the axis by removing the Dove prism and the half-wave plates and interferometrically aligning the cavity with the seed. We then insert the Dove prism and the half-wave plates and initially observe cavity resonances corresponding to one, two, or four cavity passes. We eliminate all but the one-pass fringe by optimizing the position and angle of the prism. We then align the pump beam so that it is parallel to the cavity axis. Once oscillation occurs, we verify collinear phase matching by monitoring the spatial overlap of the signal seed and the transmitted pump beams on a far-field CCD camera.

Figure 2 shows a comparison of the contours of the far-field signal fluence with and without the Dove prism in the cavity, at a pump fluence of approximately 4× threshold. Without the prism, the far-field angle is more constrained in the walk-off direction than in the orthogonal direction because of the limited acceptance angle of the crystal. With the prism in place, the beam is more symmetric, with the angular spread in both directions approximately equal to the spread in the walk-off direction without the prism.

To provide a more-quantitative characterization of the signal beam for comparison with our numerical model,[2] we measured the beam quality factors M_w^2 and M_p^2 for both the image-rotated and the

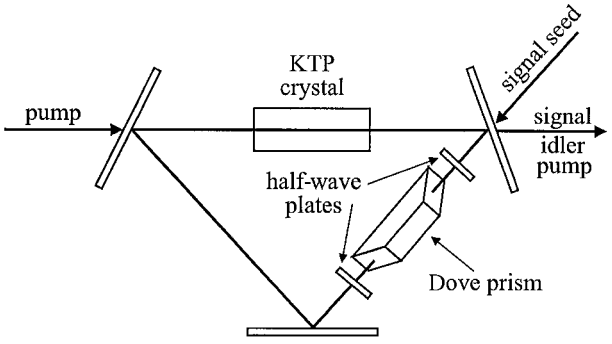

Fig. 1. Image-rotating cavity. Signal walk-off in the KTP crystal is in the cavity plane. The Dove prism is rotated 45° from the plane of the mirrors. Half-wave plates rotate the polarization of the signal to p polarization of the Dove prism.

0146-9592/02/010040-03$15.00/0

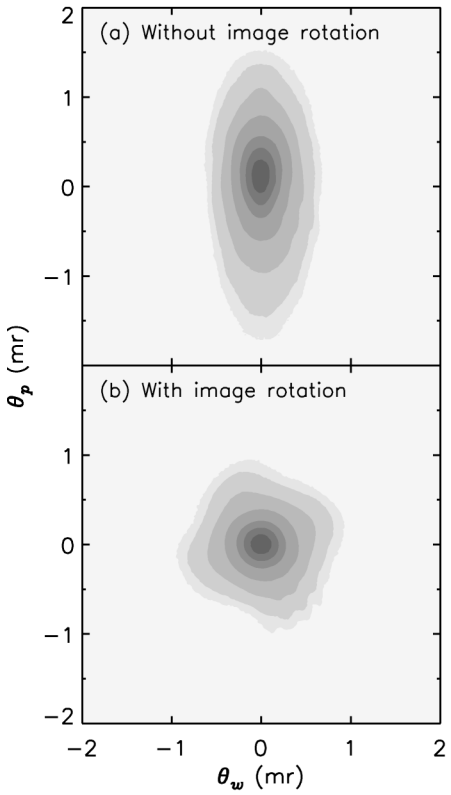

Fig. 2. Far-field signal-fluence profiles (a) without and (b) with the Dove prism, at a pump fluence of ~4× threshold. The profiles are averages of ten pulses with the background subtracted.

non-image-rotated OPOs. Subscripts w and p refer to the walk-off direction and the direction perpendicular to walk-off. Figure 3 shows predicted ${M_w}^2$ and ${M_p}^2$ with and without image rotation as a function of pump energy, along with the associated predicted signal energy. The calculations assume equal cavity lengths for the rotated and nonrotated cavities. The squares with error bars denote measured M^2 values, at a pump energy of 14 mJ, which is approximately 4× threshold. The predicted energy curves agree quite well with the experimental values (not shown), only slightly overestimating the measured efficiency. It is evident that there is only a slight efficiency penalty associated with image rotation. All the data in Fig. 3 are for the pump beam positioned to cross the signal beam midway along the crystal, the positioning that gives the lowest threshold.

M^2 is difficult to measure and model accurately. We checked the convergence of our model's predictions by increasing the number of mesh points in the transverse grid. Convergence was acceptable for grids of 128×128. Additionally, for pulsed operation, one must compute an M^2 that is characteristic of the entire pulse from a wave front that evolves significantly during the pulse. We used the adaptation of Siegman's method[3] to pulsed beams that was outlined in an earlier paper.[2] Our measured M^2 values were determined from the second moments ${\sigma_w}^2(z)$ and ${\sigma_p}^2(z)$ of the two-dimensional signal-fluence profiles recorded at various longitudinal positions spanning the waist formed by a focusing lens. We used a 10-bit, digital, progressive-scan CCD camera (Cohu 6612-3000) with electronic shutters and a pixel spacing of 9.9 μm in both directions. Externally triggering the camera in asynchronous mode resulted in simultaneous integration of all pixels within a 250-μs acquisition window. This short integration time, combined with the 10-bit digitization, allows quieter, higher-resolution measurements than those obtained from conventional analog camera beam-profiler systems. Nevertheless, obtaining accurate ${\sigma_w}^2$ and ${\sigma_p}^2$ values requires care because they are extremely sensitive to noise in the wings as a result of the w^2 and p^2 weighting of the second moments. To reduce the effects of random electronic camera noise, we recorded ten background and ten fluence profiles at each of 17 points along z. During analysis, the ten fluence profiles were repositioned to have a common centroid and then averaged. The background was averaged and subtracted from the average fluence before ${\sigma_w}^2(z)$ and ${\sigma_p}^2(z)$ were calculated. These average values accurately represent single-shot values because injection seeding the OPO and pumping at ≥4× threshold produces stable, reproducible spatial fluence profiles with rms fluctuations in energy of ≤1%. We determined the error bars on M^2 by varying the size of the rectangular area of CCD pixels, called an area of interest (AOI), within which ${\sigma_w}^2(z)$ and ${\sigma_p}^2(z)$ are calculated. For a perfect Gaussian beam and with no noise, M^2 has little dependence on AOI size as long as it is large enough to encompass the entire spatial profile. In practice, M^2 does depend on AOI size, so we report a most likely value, with an uncertainty determined by variation of the AOI size. We validated our procedure by obtaining $1.01 \leq M^2 \leq 1.05$ for pulsed and cw beams emerging from a 2-m-long single-mode optical fiber, with the waist formed by a high-numerical-aperture multielement lens (Melles Griot 06GLC001).

It is clear from the comparison of measured and predicted values of M^2 shown in Fig. 3 that agreement between the model and the experiment is quite good. In an earlier paper,[2] the model predictions of M^2 for

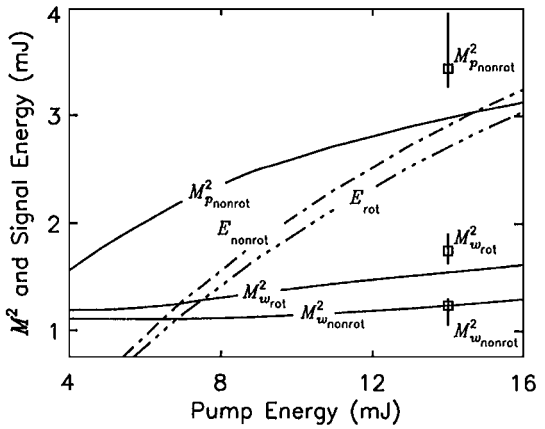

Fig. 3. ${M_w}^2$, ${M_p}^2$, and signal energy for rotated and nonrotated OPOs as a function of pump energy. Solid curves, calculated M^2; boxes, measured M^2. ${M_p}^2$ and ${M_w}^2$ are nearly equal for the image-rotated OPO. Dashed–dotted curves, calculated signal energies.

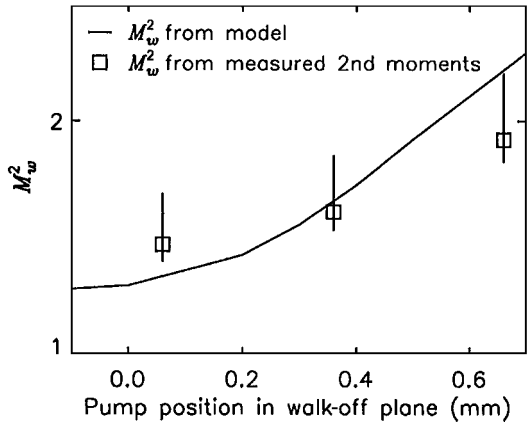

Fig. 4. Calculated and measured $M_w{}^2$ as functions of pump-beam displacement in the walk-off plane for the image-rotated OPO. The pump fluence is $\geq 4\times$ threshold.

the nonrotating OPO were validated, so agreement in that case was expected. The points that we emphasize here are that our model also predicts the performance of the image-rotated OPO quite well and that the beam quality of the image-rotated OPO in both directions is nearly as good as that of the nonrotated OPO in the walk-off direction.

Because of the asymmetry introduced by birefringent walk-off in the image-rotated OPO, it is not obvious that positioning the pump beam for minimum threshold also gives the best beam quality. We studied the influence of displacing the pump beam slightly in the walk-off direction. The calculated and measured values shown in Fig. 4 indicate that beam quality can be improved somewhat by displacement of the pump so that its greatest overlap with the signal occurs near the input end of the crystal rather than midway through the crystal. On the horizontal axis of Fig. 4, the pump and signal beams overlap midway through the crystal for a value of 0.36 mm and overlap at the input face for a value of 0.0 mm. Near 0.0 mm we find that M^2 is improved to $\lesssim 1.5$ in both directions, whereas the reduction in signal energy is only $\sim 10\%$.

Our OPOs are only $\sim 25\%$ efficient because of the relatively long cavity. However, the Fresnel number is large at $\gtrsim 15$, so our beam quality is outstanding compared with that of other nanosecond OPO designs. Additionally, our model indicates that beam quality should improve slightly with larger pump-beam diameters and higher cavity Fresnel numbers, contrary to expectations for OPOs without image rotation.

In summary, we have verified that injection-seeded, image-rotating, nanosecond OPOs can generate high-quality, symmetric beams. The OPOs that we studied had relatively low efficiencies because of their long cavities. However, shorter cavities are possible and should yield higher conversion efficiency with no reduction in beam quality. Although we do not report M^2 values for unseeded operation, we observed high beam quality, although the oscillation threshold was higher and efficiency lower than for seeded operation. Finally, we note that the beam from the image-rotated OPO has a nearly perfect Gaussian core surrounded by a small shoulder. Knowing our measurement and analysis procedures can yield $M^2 \sim 1$ with a nearly perfect validation beam, we attribute our measured $M^2 > 1.5$ primarily to this small shoulder. In fact, using other methods for measuring M^2 that are not as sensitive to the small shoulder, such as the commonly used knife-edge method,[4] we find M^2 of 1.04, 1.11, 1.27 for the beams in Fig. 4.

This work was supported by the U.S. Department of Energy under contract DE-AC04-94AL85000. Sandia is a multiprogram laboratory operated by Sandia Corporation, a Lockheed Martin Company, for the U.S. Department of Energy. D. J. Armstrong's e-mail address is darmstr@sandia.gov.

References

1. A. V. Smith and M. S. Bowers, "Image-rotating cavity designs for improved beam quality in nanosecond optical parametric oscillators," J. Opt. Soc. Am. B **18,** 706–713 (2001).
2. A. V. Smith, W. J. Alford, T. D. Raymond, and M. S. Bowers, "Comparison of a numerical model with measured performance of a seeded, nanosecond KTP optical parametric oscillator," J. Opt. Soc. Am. B **12,** 2253–2267 (1995).
3. A. E. Siegman, "Defining the effective radius of curvature for a nonideal optical beam," IEEE J. Quantum Electron. **27,** 1146–1148 (1991).
4. T. F. Johnston, "Beam propagation (M^2) measurement made as easy as it gets: the four-cuts method," Appl. Opt. **37,** 4840–4850 (1998).